Journal of Solid State Chemistry 181 (2008) 2869–2876

Contents lists available at ScienceDirect

Journal of Solid State Chemistry

journal homepage: www.elsevier.com/locate/jssc

Processing and characterization of new oxysulfide glasses in the Ge–Ga–As–S–O system

C. Maurel [a,b], L. Petit [a,*], M. Dussauze [c], E.I. Kamitsos [c], M. Couzi [d], T. Cardinal [b], A.C. Miller [e], H. Jain [e], K. Richardson [a]

[a] School of Materials Science and Engineering, Clemson University, COMSET, 161 Sirrine Hall, Box 340971, Clemson, SC 29634, USA
[b] Institut de Chimie de la Matière Condensée de Bordeaux, CNRS-Université Bordeaux 1, 87 Av. Dr. Schweitzer, 33608 Pessac, France
[c] Theoretical and Physical Chemistry Institute, National Hellenic Research Foundation, 48 Vass. 116 35 Athens, Greece
[d] Institut des Sciences Moléculaires, UMR 5255 CNRS, Université Bordeaux 1, 351 Cours de la Libération, 33405 Talence, France
[e] Center for Optical Technologies and Department of Materials Science and Engineering, Lehigh University, 5E Packer Avenue, Bethlehem, PA 18015, USA

ARTICLE INFO

Article history:
Received 8 May 2008
Received in revised form
20 June 2008
Accepted 15 July 2008
Available online 22 July 2008

Keywords:
Oxysulfide
Raman and IR spectroscopies
XPS

ABSTRACT

New oxysulfide glasses have been prepared in the Ge–Ga–As system employing a two-step melting process which involves the processing of the chalcogenide glass (ChG) and its subsequent melting with amorphous GeO_2 powder. Optical characterization of the synthesized oxysulfide glasses has shown that the cut-off wavelength decreases with increasing oxygen content, and this has been correlated to results of Raman and infrared (IR) spectroscopies which show the formation of new oxysulfide structural units. X-ray photoelectron spectroscopy (XPS) analysis to probe the bonding environment of oxygen atoms in the oxysulfide glass network, has revealed the preferred formation of Ga–O and Ge–O bonds in comparison to As–O bonds. This work has demonstrated that melting a ChG glass with GeO_2 leads to the formation of new oxysulfide glassy materials.

1. Introduction

Despite their often limited thermal and mechanical stability, attributable to weaker bond strengths and thus lower glass transition temperatures, chalcogenide glasses (ChG) have attracted attention as candidate materials in nonlinear optical applications at telecommunication wavelengths [1] due to their higher nonlinear optical response than oxide glasses [2]. However, the number of their practical applications has been found to be consequently reduced due to their high photo-sensitivity to light exposure in the visible and the near-infrared (NIR) spectral range leading to the need of new glasses development. Oxysulfide materials, which are expected to have a better chemical stability toward exposure to visible and NIR light in comparison with the corresponding sulfide glasses, should also offer the possibility of combining the mechanical properties of oxide materials with the attractive optical traits of sulfide glasses by adjusting the sulfur to oxygen ratio. Despite the limited studies on oxysulfide glasses for optical applications, it has been reported in [3] that these newly developed glasses are, also, more resistant to atmospheric attack than the corresponding sulfide glasses.

Germanium oxide-based glasses containing heavy metal oxides have been more widely investigated for infrared (IR) device applications [4] than germanium oxysulfide glass systems [5,6]. Even though these systems exhibit broad glass-forming regions, there are still remaining challenges related to the definition of suitable processing or elaboration routes. Kim et al. [6] have shown that germanium oxysulfide glasses can be prepared in the system $(1-x)GeS_2$–$xGeO_2$ for $0<x<1$, by rapidly quenching melts to room temperature with no evidence of phase separation across the entire compositional range. However, recently, Terakado et al. explained that the Ge:S ratio can deviate from GeS_2 by ~10 at%, depending critically upon the preparation conditions [7]. The oxysulfide glasses in the system GeS_2–GeO_2, elaborated using melt quench technique, have been proposed to be heterogeneous over a nano-scale due to phase separation phenomenon [7]. We demonstrated that a sulfination heat treatment of GeO_2 powder can also lead to the formation of germanium-based oxysulfide powder. Raman spectroscopy was a useful tool to show the presence of new modes that were assigned to intermediate germanium oxysulfide structural units. Moreover, we have shown that it is possible to deposit amorphous films in the GeS_2–GeO_2 system using a RF sputtering technique which can be considered as a fast quenching rate as compared to classical melt quench technique [8].

The aim of this study is to investigate an alternative technique to process oxysulfide glasses using a two-step process. In this

* Corresponding author.
E-mail address: lpetit@clemson.edu (L. Petit).

0022-4596/$ - see front matter Crown Copyright © 2008 Published by Elsevier Inc. All rights reserved.
doi:10.1016/j.jssc.2008.07.019

current study, the glasses in the Ge–Ga–As–S–O system are processed with an excess of S and with a low As content to possess good physical stability and high nonlinear index. To create a matrix amenable to rare-earth doping in the germanate glass network, a limited fraction of germanium atoms can be replaced by gallium where Ga_2S_3 acts as co-former. Indeed, it has been found that, unlike Ge–Sb–S glasses, Ge–Ga–S glasses are good host materials for incorporation of rare-earths since they have been shown to be capable of dissolving relatively larger amounts of rare-earth elements [9].

This paper reports on the processing and characterization of these new germanium-based oxysulfide glasses using a standard melting method for ChG glasses. The structural changes induced by the addition of oxygen, introduced through melting of amorphous GeO_2 with Ge–As–S and Ge–Ga–As–S glasses, have been systematically investigated using Raman and IR spectroscopies as well as X-ray photoelectron spectroscopy (XPS). Investigating the effect of compositional modifications on the glass network structure will be of importance for understanding of the linear and nonlinear optical properties later.

2. Experimental

Germanium oxysulfide bulk glasses were prepared with different O/S ratios using a two-step melting process in order to determine the maximum concentration of oxygen that can be incorporated without crystallization or phase separation. The first step consisted of the processing of the chalcogenide glass which was then re-melted, in the second step, with amorphous GeO_2 powder. The chalcogenide-based glasses with compositions $Ge_{23}As_7S_{70}$ and $Ge_{18}Ga_5As_7S_{70}$ were prepared in 20 g batches using high purity elements and compounds (As and Ge: Aldrich 99.999%, S: Cerac 99.999% and Ga_2S_3: Aldrich 99.99%). Starting materials were weighed and batched into quartz ampoules inside a nitrogen-purged glove box and sealed under vacuum using a gas–oxygen torch. Prior to sealing and melting, the ampoule and batch were pre-heated at 100 °C for 4 h to remove potential surface moisture from the quartz ampoule and the batch raw materials. The ampoule was then sealed and heated for 24 h at 925 °C. A rocking furnace was used to rock the ampoule and increase the homogeneity of the melt. Once homogenized, the melt-containing ampoule was air-quenched to room temperature. To avoid fracture of the tube and glass ingot, the ampoules were subsequently returned to the furnace for annealing for 15 h at 40 °C below the glass transition temperature, T_g. The composition of the glasses was analyzed using energy dispersive spectroscopy (EDS). Within the accuracy of measurements ($\pm$2% for Ge, Ga, As, S; $\pm$5% for O), no oxygen was found in the prepared chalcogenide glasses.

The oxysulfide glasses were prepared by melting in vacuum 3 g of the chalcogenide glasses with powder of amorphous GeO_2 (Cerac 99.999%) in graphite crucibles placed inside a quartz ampoule. Three different systems were synthesized: the systems $(1-x)Ge_{23}As_7S_{70}-xGe_{33}O_{67}$ with $x=0$ and 0.10, and $(1-y)Ge_{18}Ga_5As_7S_{70}-yGe_{33}O_{67}$ with $y=0$ and 0.32, leading to an increase of the Ge content, and $Ge_{18}Ga_5As_7S_{(70-z)}O_z$ with $z=5$ and 12.5 to keep the ratio between glass-forming cations similar. Prior to melting, the ampoule was sealed under vacuum. The melting temperature of 925 °C was reached with a 2.5 °C/min heating ramp without rocking the furnace. After quenching, the oxysulfide glass was removed from the graphite crucible and then annealed in air at 150 °C for 15 h. The oxysulfide glasses were stored in a dry nitrogen environment within a glove box prior to use. The samples were then cut, optically polished and inspected visually. Some carbon contamination, most probably from the graphite crucible, could be observed and was confirmed using EDS which also allows the verification of the presence of oxygen in the oxysulfide glasses. The quantification of oxygen content is not expected to be accurate due to the accuracy of the EDS measurement.

The glass transition temperature (T_g) was determined by Differential Scanning Calorimetry (DSC) at a heating rate of 10 °C/min from 50 to 500 °C using a commercial apparatus (TA Instruments Inc.). The measurements were carried out in a hermetically sealed aluminum pan. The glass transition temperature was taken at the inflection point of the endotherm, as obtained by taking the first derivative of the DSC curve, and T_g was determined with an accuracy of $\pm$5 °C.

The density of glasses was measured by the Archimedes' principle using diethylphthalate as the immersion liquid, with an accuracy of $\pm 0.02\ g/cm^3$.

The visible–near-infrared (Vis–NIR) absorption spectra were measured at room temperature on 2 mm thick optically polished samples.

Raman spectra were recorded at room temperature on a LabRam confocal micro-Raman instrument (Jobin-Yvon), using backscattering geometry and a typical resolution of 2–3 cm^{-1}. The system consists of a holographic notch filter for Rayleigh rejection, a microscope equipped with 10×, 50× and 100× objectives (the latter allowing a spatial resolution of less than 2 μm), and a CCD detector. The 752 nm emission line of an argon–krypton laser was used for excitation with incident power of around 10 mW. The use of a 752 nm source was essential to this study because this excitation wavelength was well below the bandgap region for most of the studied samples.

Infrared spectroscopic measurements were performed at room temperature on a Fourier-transform vacuum spectrometer (Bruker 113 V) fully equipped with two detectors and five different beam splitters to cover the frequency range from 30 to 5000 cm^{-1}. Infrared reflectance spectra were measured at quasi normal incidence (11°), with each spectrum resulting from the average of 400 scans acquired at a typical resolution of 2 cm^{-1}. The complex refractive index of glasses was obtained through Kramers-Kronig analysis of the measured specular reflectance spectra [10], and this allowed for the calculation of the absorption coefficient spectra, α, through the relation:

$$\alpha = 4\pi\nu k(\nu) \quad (1)$$

where ν is the frequency (in cm^{-1}) and $k(\nu)$ is the frequency-dependent imaginary part of the complex refractive index.

The XPS spectra of $Ge_{18}Ga_5As_7S_{(70-z)}O_z$ with $z=5$ and 12.5 were obtained on samples fractured in situ in the analysis chamber using a hard tool. A Scienta 300 ESCA instrument was employed for XPS measurements at a vacuum of 10^{-9} Torr (Zettlemoyer Center for Surface Studies, Lehigh University). A monochromatic Al X-ray source was used for the analysis, and a low energy electron flood gun was used to minimize surface charging. Survey spectra were recorded from 0 to 1250 eV with pass energy of 150 eV using 1 eV/0.3 s steps in 1 scan. Individual high resolution spectra of As 3*d*, Ge 3*d*, and Ga 2*p* were recorded with a pass energy of 150 eV, in 0.05 eV/0.3 s steps. The number of scans was between 2 and 10, depending on the intensity of the peak, to reach a satisfactory signal/noise ratio. ESCA analysis software from Scienta Instrument was used to facilitate peak deconvolution [Gammadata Scienta AB P.O. Box 15120 SE-750 15 Uppsala, Sweden]. The low resolution XPS scan from the sample with $z=5$, taken as an example, is shown in Fig. 1. The core level peaks and X-Ray induced Auger lines from the constituent elements are easily identified and marked on the spectrum.

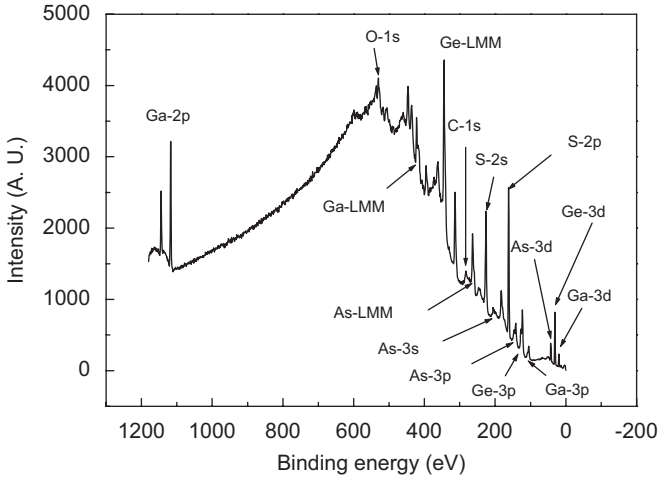

Fig. 1. Low resolution XPS spectrum obtained for the glass $Ge_{18}Ga_5As_7S_{70-z}O_z$ with $z = 5$.

3. Results and discussion

The aim of this study is to investigate the processing and characterization of new Ge–Ga–As–S–O oxysulfide glasses for optical applications. Raman, IR and XPS spectroscopies have been employed to track and evaluate structural modifications caused by the systematic substitution of O for S.

Germanium-based oxysulfide glasses with compositions $(1-x)Ge_{23}As_7S_{70}-xGe_{33}O_{67}$ with $x = 0.10$, and $(1-y)Ge_{18}Ga_5As_7S_{70}-yGe_{33}O_{67}$ with $y = 0.32$ have been prepared by melting ChG glasses with amorphous GeO_2 powder. Some gallium-containing chalcogenide glasses have been prepared deficient in germanium in order to keep the Ge/Ga/As ratios constant in the oxysulfide glasses with compositions $Ge_{18}Ga_5As_7S_{(70-z)}O_z$ where $z = 5$ and 12.5. Note that for the calculation of the resulting oxysulfide atomic percents, GeO_2 is expressed in molar fraction as $Ge_{33}O_{67}$. In the following, we will focus our discussion on the evolution of IR, Raman and XPS spectral features which are informative of local bonding in the glass network, to understand the correlations between structural characteristics and optical or mechanical properties of such glasses.

3.1. Effect of oxygen introduction on the structure of gallium-free glasses

Oxysulfide glasses have been obtained by incorporating amorphous GeO_2 in the $Ge_{23}As_7S_{70}$ glass network. The oxygenated glasses were very brittle and broke into small pieces during the quench. The composition of the prepared glasses has been determined using EDS. In the oxysulfide glasses, carbon was detected but no clear relation has been observed between the glass composition and carbon content. The presence of carbon was attributed to some contamination from the graphite crucible. Table 1 gives the nominal glass compositions and those obtained from the EDS analysis (without considering carbon contamination). Larger contents of oxygen were obtained in the prepared glasses as compared to the batch compositions, suggesting that oxygen contamination occurred during the second step of preparation of the oxysulfide glasses. The density and glass transition temperature of glasses are summarized also in Table 1. No density value for the $(1-x)Ge_{23}As_7S_{70}-xGe_{33}O_{67}$ glass with $x = 0.10$ is reported, as it was not possible to prepare this composition in dimensions sufficient for accurate measurements. One can note that the glass transition temperature (T_g) increases dramatically when GeO_2 is introduced. This increase may be related not only to the incorporation of oxygen but also to the increase of germanium content.

The absorption spectra of glasses are shown in Fig. 2A. Fresnel reflections have been subtracted by taking into account that the chalcogenide and oxysulfide glasses exhibit weak absorption around 800 nm. Because of the small size of the investigated oxysulfide glasses prepared in the system $(1-x)Ge_{23}As_7S_{70}-xGe_{33}O_{67}$, glass specimens were glued on a microscope slide for the measurement (note that glue shows no absorption in the 500–800 nm range). Fig. 2A shows that the absorption edge shifts progressively to smaller wavelengths when the oxygen content increases in glasses.

The Raman spectra of the investigated glasses, presented in Fig 3A, exhibit a broad band with a maximum near 340 cm^{-1} and smaller bands near 475 cm^{-1}. The broad band near 340 cm^{-1} is formed by the overlap of multiple contributing Raman signals. The shoulder at around 300 cm^{-1} has been assigned to the E modes of $SbS_{3/2}$ pyramids. In agreement with [11–15], the bands at 330 and 400 cm^{-1} have been assigned to the A_1 and T_2 modes of corner-sharing $GeS_{4/2}$ groups with a smaller contribution of the $\nu_1(A_1)$ mode of $AsS_{3/2}$ pyramids (observed at 344 cm^{-1} for As_2S_3 glass [13–16]). The bands at 340, 375 and 420 cm^{-1} have been attributed, respectively to A_1 mode of the GeS_4 molecular units, to the T_2 mode of 2 edge-sharing $Ge_2S_4S_{2/2}$ tetrahedra and to the vibration of two tetrahedral connected through a bridging sulfur $S_3Ge–S–GeS_3$. The excess of sulfur in the glass is expected to be manifested by Raman bands at higher wavenumbers. Thus, the band at 425 cm^{-1} can be attributed to the vibrations of two tetrahedra connected through one bridging sulfur atom, as in $S_3Ge–S–GeS_3$, while the lower intensity band at ca. 475 cm^{-1} may be attributed to the $S_8(A_1)$ ring vibration mode and at 485 cm^{-1} to vibration mode of $S(A_1)$ chain. [11–14]. The frequencies and the corresponding assignments are summarized in Table 2. It is possible to think that the re-melting of the ChG glass with GeO_2 powder leads to some loss of sulfur revealed in the Raman spectrum of Fig. 3A by a decrease of the 475 cm^{-1} band amplitude. Sulfur is no more in excess in the oxysulfide glass. Moreover, as seen in Fig. 3A, the main band becomes broader and shifts to higher wavenumber when GeO_2 is introduced in the $Ge_{23}As_7S_{70}$ network. The increase in intensity at ca. 375 cm^{-1} in the spectrum of the oxysulfide glass should indicate an increase in the ratio of edge-sharing to corner-sharing $GeS_{4/2}$ tetrahedra. Thus, Raman spectroscopy indicates changes in the interconnectivity between $GeS_{4/2}$ tetrahedra, involving now a greater number of edge-sharing tetrahedra. Because of the presence of oxygen atoms in the glass network, one can expect contributions from the symmetric stretching of Ge–O–Ge bridging bonds around 420 cm^{-1} [20]. In accordance with our recent study on a more simple system such as $GeS_2–GeO_2$ [8], the main band cannot be obtained by simple summation of GeS_2 vibrational features to the oxide spectra. The addition of a new band between 360 and 400 cm^{-1}, different from GeO_4 or GeS_4 tetrahedral sites, was necessary to correctly simulate the spectrum. As we explained [8], such vibrations could be related to the formation of species such as GeO_3S, GeO_2S_2 or $GeOS_3$ tetrahedral units in agreement with Kim et al. who suggested that germanium atoms are coordinated with both sulfur and oxygen [6].

In order to complement the structural analysis, IR spectra of the glasses have been measured and are presented in Fig. 4A. The spectra show a dominant feature at 380 cm^{-1} which can be related to the $\nu_3(F_2)$ mode of corner-sharing $GeS_{4/2}$ with a shoulder at ca. 325 cm^{-1} which can be attributed to contributions from the $\nu_3(E)$ mode of $AsS_{3/2}$ pyramids expected at 310 cm^{-1} [16–19] and from the $\nu_1(A_1)$ mode of corner-sharing $GeS_{4/2}$ tetrahedral units. The weak band at 155 cm^{-1} should be due mainly to the bending mode $\nu_4(F_2)$ of $GeS_{4/2}$ tetrahedral units

Table 1
Nominal and analyzed composition, density and glass transition temperature (T_g) of the investigated oxysulfide glasses in the system Ge–Ga–As–S–O

Batch composition of glasses	Analyzed composition by EDS (±2% for Ge, Ga, As, S) (±5% for O)	Density (g/cm^3) (±0.02 g/cm^3)	T_g (°C) (±5 °C)
$(1-x)Ge_{23}As_7S_{70}+xGe_{33}O_{67}$			
$x = 0$ $Ge_{23}As_7S_{70}$	$Ge_{23}As_7S_{70}$	2.80	317
$x = 0.10$ $Ge_{24}As_6S_{63}O_7$	$Ge_{26}As_7S_{58}O_9$	NA	390
$(1-y)$ $Ge_{18}Ga_5As_7S_{70}+xGe_{33}O_{67}$			
$y = 0$ $Ge_{18}Ga_5As_7S_{70}$	$Ge_{16}Ga_5As_9S_{70}$	2.87	286
$y = 0.32$ $Ge_{23}Ga_3As_5S_{48}O_{21}$	$Ge_{24}Ga_5As_5S_{41}O_{31}$	2.74	392
$Ge_{18}Ga_5As_7S_{70-z}O_z$			
$z = 5$ $Ge_{18}Ga_5As_7S_{65}O_5$	$Ge_{20}Ga_7As_8S_{58}O_7$	2.93	328
$z = 12.5$ $Ge_{18}Ga_5As_7S_{57}O_{13}$	$Ge_{20}Ga_8As_7S_{50}O_{16}$	3.00	338

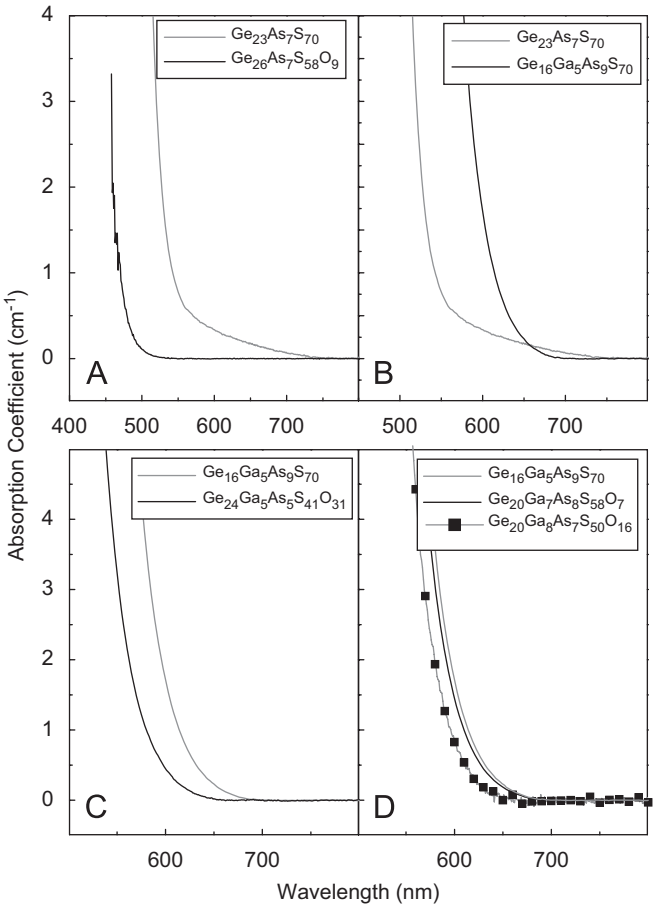

Fig. 2. Absorption spectra of glasses in the systems: $(1-x)Ge_{23}As_7S_{70}+xGe_{33}O_{67}$ (A), gallium-free and gallium-containing sulfide samples (B), $(1-y)Ge_{18}Ga_5As_7S_{70}+yGe_{33}O_{67}$ (C) and $Ge_{18}Ga_5As_7S_{70-z}O_z$ (D). Glass compositions are the analyzed compositions in Table 1.

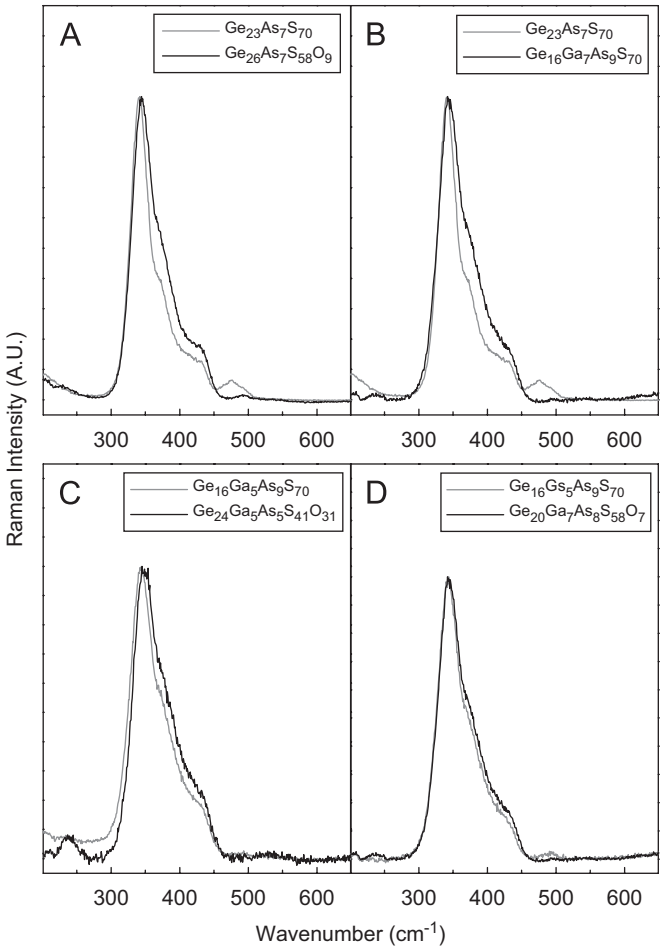

Fig. 3. Raman spectra of glasses in the systems: $(1-x)Ge_{23}As_7S_{70}+xGe_{33}O_{67}$ (A), gallium-free and gallium-containing sulfide samples (B), $(1-y)Ge_{18}Ga_5As_7S_{70}+yGe_{33}O_{67}$ (C) and $Ge_{18}Ga_5As_7S_{70-z}O_z$ (D). Glass compositions are the analyzed compositions in Table 1.

[16–19]. Introduction of oxygen atoms causes more pronounced changes in the IR spectrum as shown by the new bands at 250, 530 and 820 cm^{-1} (Fig. 4A). By analogy with vibration modes observed for glassy and crystalline As_2O_3, one can attribute the band at 530 cm^{-1} to the stretching vibration of As–O bonds [21,22]. The band at 820 cm^{-1} can be related to the asymmetric stretching vibration of Ge–O–Ge bonds, while the corresponding bending mode is expected in the 200–350 cm^{-1} spectral range [20]. It should be noted that for pure GeO_2 glass the asymmetric stretching of Ge–O–Ge bridges is measured at 915 cm^{-1} [20]. The frequencies and the corresponding ones are also summarized in Table 2.

In summary, the Raman and IR spectra show that introduction of GeO_2 in the Ge–As–S glass induces changes in the interconnectivity of GeS_4 tetrahedra due to variations in the sulfur content, leading probably to the formation of new oxysulfide units such as $GeOS_3$, GeO_2S_2 or GeO_3S. These structural changes are consistent with the blue-shift of the absorption edge observed in Fig. 2A, the increase of T_g (Table 1) and the strengthening of the glass network through participation of oxygen atoms in bond formation.

Table 2
Assignments of infrared and Raman frequencies (cm^{-1}) of the investigated glasses

Frequency (cm^{-1}) IR	Frequency (cm^{-1}) Raman	Assignments
155		F_2 mode of corner-sharing $GeS_{4/2}$ [16–19]
250–300		Bending mode of Ge–O–Ge bonds [20].
300	300	E modes of $SbS_{3/2}$ pyramids
	240	$S_3Ge–GeS_3$ structural units [23–25]
325	330	A_1 mode of corner-sharing $GeS_{4/2}$ [11–19], A_1 (Raman)/E (IR) mode of $AsS_{3/2}$ pyramids [13–19]
	340	A_1 mode of the GeS_4 and GaS_4 molecular units [11–15]
	375	T_2 mode of two edge-sharing $Ge_2S_4S_{2/2}$ [11–15], A_1^c companion [GeS_4] and A_1^c companion [GaS_4]
380		F_2 mode of corner-sharing $GeS_{4/2}$ [16–19]
	400	T_2 mode of corner-sharing $GeS_{4/2}$ and $GaS_{4/2}$ [11–15]
	Shoulder at 420	$S_3Ge–S–GeS_3$ [11–15], Ge–O–Ge bridging bonds [20]
	475	A_1 mode of S_n ring [11–14]
	485	A_1 mode of S_n chain [11–14]
530		Stretching vibration of As–O [21,22]
680		Ga–O bonds [28,29]
820		Asymmetric stretching vibration of Ge–O–Ge bonds [20]

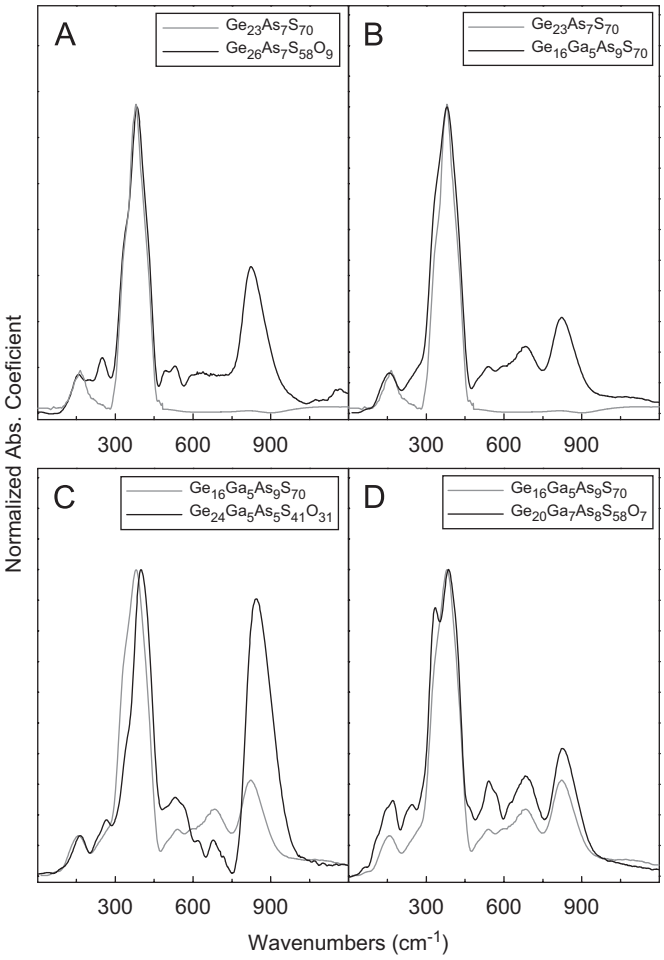

Fig. 4. Normalized infrared absorption spectra of glasses in the system: $(1-x)Ge_{23}As_7S_{70}+xGe_{33}O_{67}$ (A), gallium-free and gallium-containing sulfide samples (B), $(1-y)Ge_{18}Ga_5As_7S_{70}+yGe_{33}O_{67}$ (C) and $Ge_{18}Ga_5As_7S_{70-z}O_z$ (D). Glass compositions are the analyzed compositions in Table 1.

3.2. Effect of oxygen introduction on the structure of gallium-containing glasses

Before discussing the effect of O incorporation on some of the optical and structural properties of the gallium-containing glasses, the effect of Ga in the germanium-based network on the optical and structural properties of the glasses is first described.

As seen in Table 1, replacement of Ge by Ga in the original composition $Ge_{23}As_7S_{70}$ to form $Ge_{18}Ga_5As_7S_{70}$ induces a decrease in T_g and an increase in density. These changes in properties indicate a weakening of the glass network, due probably to gallium participation in the glass network. In parallel, Fig. 2B shows a corresponding red shift of the absorption band edge with gallium incorporation which is consistent with the density increase.

Gallium is known to form $GaS_{4/2}$ tetrahedral units connected through bridging sulfur atoms. The frequencies of the fundamental vibration modes of $GaS_{4/2}$ units are very close to those of $GeS_{4/2}$ tetrahedra because of similarities in the electronic configuration and atomic mass of the two glass-forming cations Ge and Ga [23–26]. For the glasses under investigation, the vibrational spectra are more likely to be dominated by responses of germanium-based units because of the small Ga content. However, it is noted that the deficiency of Ga_2S_3 in sulfur would cause several effects on the local structure when this compound is added to a GeS_2-based glass matrix. Thus, an early EXAFS study revealed structural modifications by formation of edge linkages in place of corner linkages between the tetrahedral units [27], while Raman spectroscopy suggested the formation of Ge–Ge bonding in $S_3Ge–GeS_3$ unit as a structural alternative to compensate for the sulfur deficiency [23–25]. Such units have been also proposed by Lucovsky et al. [11] in sulfur deficient $Ge_{1-x}S_x$ glasses, with a characteristic Raman signature at 240 cm^{-1}.

As shown in Fig. 3B, introduction of gallium in the germanate network induces several Raman spectral changes including the disappearance of the 475 cm^{-1} band and the parallel increase in intensity of the shoulder at 375 cm^{-1} suggesting the increase of the relative population of edge-sharing $GeS_{4/2}$ or $GaS_{4/2}$ tetrahedral, respectively. Moreover, the spectrum of the Ga-containing glass exhibits a weak band at 240 cm^{-1}, which could be related to the formation of the $S_3Ge–GeS_3$ structural unit. These findings suggest that gallium introduction induces an increase in the proportion of edge-sharing tetrahedral units.

In the presence of gallium, the IR spectra show new absorption bands at ca. 530, 680 and 820 cm^{-1} (Fig. 4B). By analogy with the assignments proposed for the $Ge_{26}As_7S_{58}O_9$ oxysulfide glass, the bands at 530 and 820 cm^{-1} can be related to stretching modes of As–O and Ge–O bonds, respectively. Following [28,29], the band at 680 cm^{-1} should indicate the existence of Ga–O bonds in the glass network. The presence of oxygen in the $Ge_{18}Ga_5As_7S_{70}$ glass should be related to contamination of the Ga_2S_3 powder used in glass preparation. Besides spectral effects caused by oxygen contamination, the Ga-containing glass shows a broadening of the main absorption at 380 cm^{-1} (Fig 4B). This effect could be due to contributions from the stretching modes of $GaS_{4/2}$ tetrahedral units and edge-sharing entities in the glass, which are superimposed on the main contribution of $GeS_{4/2}$ tetrahedra at 380 cm^{-1}.

Two different families of gallium-based oxysulfide glasses were prepared by adding GeO_2 in the $Ge_{18}Ga_5As_7S_{70}$ glass network leading to an increase of the Ge content and also in a chalcogenide glass prepared deficient in Ge to keep the ratio of cations similar. In the gallium-containing glasses, the oxysulfide glasses appear to be mechanically more stable upon casting (shock, fracture) leading to samples with larger dimensions. The introduction of larger amount of oxygen in the $(1-y)Ge_{18}Ga_5As_7S_{70}-yGe_{33}O_{67}$

glass system was possible up to $y = 0.32$. Above this value the samples were not homogeneous. For the $Ge_{18}Ga_5As_7S_{(70-z)}O_z$ glass system for which sulfur replaces for oxygen without modification of the glass-forming cation ratios, glasses of lower oxygen content have been investigated. As seen in Table 1, the density decreases with addition of GeO_2 in the $Ge_{18}Ga_5As_7S_{70}$ as expected. However, it is interesting to point that the density increases in $Ge_{18}Ga_5As_7S_{(70-z)}O_z$ oxysulfide glasses when the oxygen content increases. This may indicate that the volume of the glass decreases when oxygen is introduced in the glass network confirming the incorporation of oxygen in the glass network. As seen in the Ga-free oxysulfide glasses, the addition of GeO_2 leads also to an increase of T_g. However, it is interesting to point out that the increase of T_g is lower when oxygen is added without increasing Ge content than when it increases the Ge content. This confirms that the dramatic increase of T_g when GeO_2 is added in the other glass systems is mainly related to the increase of Ge content.

Figs. 2C and D show that the absorption edge shifts progressively to smaller wavelengths when the oxygen content increases in glasses of the systems $(1-y)Ge_{18}Ga_5As_7S_{70}-yGe_{33}O_{67}$ and $Ge_{18}Ga_5As_7S_{(70-z)}O_z$ as seen in Fig. 2A.

The Raman spectra of new glasses in the systems $(1-y)Ge_{18}Ga_5As_7S_{70}-yGe_{33}O_{67}$ and $Ge_{18}Ga_5As_7S_{(70-z)}O_z$ are presented in Figs. 3C and D, respectively. The main Raman band shifts to higher wavenumbers and becomes broader with the incorporation of oxygen. By analogy with effects discussed for the $Ge_{26}As_7S_{58}O_9$ glass, these changes can originate from the formation of edge-sharing $GeS_{4/2}$ and $GaS_{4/2}$ tetrahedra (shoulder at ca. 375 cm^{-1}) and/or mixed oxysulfide tetrahedral units GeO_3S, GeO_2S_2 or $GeOS_3$. However, compared to the changes observed in the Raman spectra of the Ga-free glasses after addition of oxygen, these variations are less distinct revealing less structure variation. Gallium-containing glasses seem to offer better ability to incorporate oxygen without strong change of the sulfide glass network.

The IR spectra of the oxysulfide glasses in Figs. 4C and D show the presence of bands at ca. 530, 680 and 820 cm^{-1}, which, as explained in the previous paragraph, confirm the development of local structural units with As–O, Ga–O and Ge–O bonds, respectively. For glass composition $Ge_{24}Ga_5As_5S_{41}O_{31}$ (Fig. 4C), no conclusion can be drawn for any preference of oxygen bonding to a specific glass-forming cation because of the large Ge content. In the case of $Ge_{20}Ga_7As_8S_{58}O_7$ glass (Fig. 4D), an enhancement is observed for the $\nu_1(A_1)$ mode of $AsS_{3/2}$ pyramids at 325 cm^{-1} relative to the corner-sharing $GeS_{4/2}$ at 380 cm^{-1}. This enhancement occurs despite the fact that the As/Ge ratio is reduced in the oxysulfide glass, suggesting that oxygen has a larger affinity for bonding to Ge and Ga in comparison to As.

Bonding trends have been studied also by X-Ray Photoelectron Spectroscopy for glasses in the system $Ge_{18}Ga_5As_7S_{70-z}O_z$. The parameters for fitting the measured XPS spectra were chosen using pure elemental data as reference and fitting optimization. A minimum number of peaks was employed to achieve reasonable fits to the data within the experimental error. Based on self-consistency of all fitting results and on our understanding of the glass system, we proposed assignments of peaks to different chemical environments. The core level 3*d* spectrum of Ge is shown in Fig. 5 for two glass compositions, where an acceptable fit of both spectra was obtained with two peaks at 31.3 and 32.3 eV. These single peaks are a convolution of the 3*d* 5/2 and 3*d* 3/2 peaks for all chemical environments, and, in accordance with our previous study [30], can be assigned to Ge bonded to S (labeled $Ge^{4+}(S)$) and to Ge bonded to O (labeled $Ge^{4+}(O)$), respectively. The As(3*d*) spectra of the same glasses in Fig. 6 have been deconvolved into two doublets for a proper fit to the data. The doublet arising from As bonded to S (labeled $As^{3+}(S)$) is located in the 43–42 eV binding energy range with a separation of

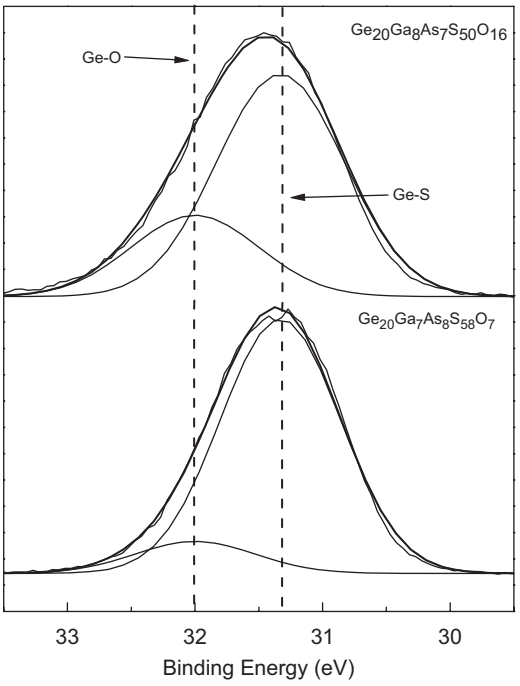

Fig. 5. High resolution XPS spectra of Ge(3*d*) as a function of oxygen content (*z*) for glasses in the system $Ge_{18}Ga_5As_7S_{70-z}O_z$. Glass compositions are the analyzed compositions in Table 1.

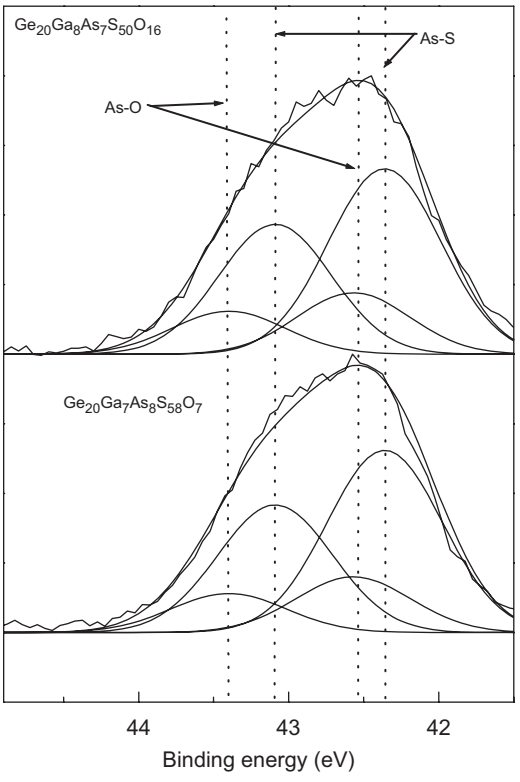

Fig. 6. High resolution XPS spectra of As(3*d*) as a function of oxygen content (*z*) for glasses in the system $Ge_{18}Ga_5As_7S_{70-z}O_z$. Glass compositions are the analyzed compositions in Table 1.

0.7 eV. The doublet observed at 43.4–42.6 eV has been assigned to As bonded to O (labeled $As^{3+}(O)$). The photoelectron spectra of Ga(2*p*) core level, displayed in Fig. 7, have been deconvoluted into two peaks. The bonding energy of Ga(2*p*) at 1118 eV was attributed to Ga bonded to S (labeled $Ga^{4+}(S)$), and the one at

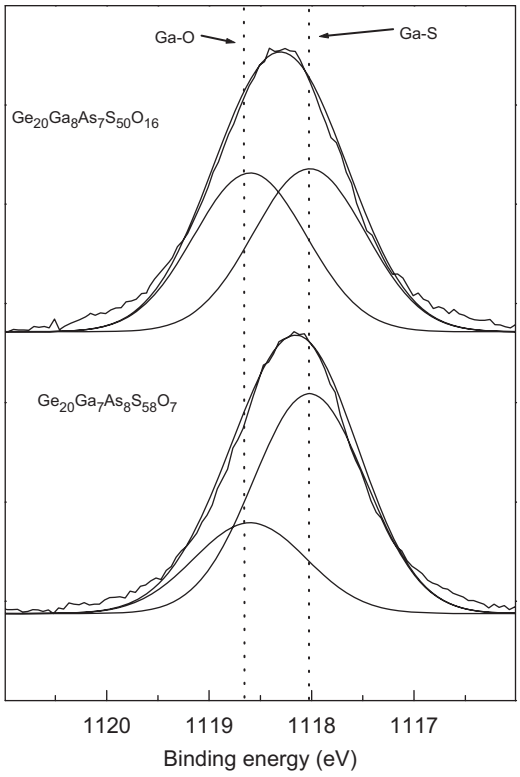

Fig. 7. High resolution XPS spectra of Ga($2p$) as a function of oxygen content (z) for glasses in the system $Ge_{18}Ga_5As_7S_{70-z}O_z$. Glass compositions are the analyzed compositions in Table 1.

higher binding energy to Ga bonded to O (labeled Ga^{4+}(O)) in accordance with Lazelle et al. [31]. The relative fractions of various species were obtained from the fitted XPS spectra, and are summarized in Table 3. The analysis of XPS spectra shown in Figs. 5–7 confirms the presence Ge–O, As–O and Ga–O bonds in the glass network, with relative proportions increasing with oxygen content (Table 3). The percentage of Ga atoms bonded to O is larger compared to that of Ge and As, with approximately 50% of Ga atoms bonded to O in the high oxygen content glass. This result may be related to the fact that the Ga–S bond is the weakest bond compared to Ge–S and As–S bonds. The numbers of Ge–O, Ga–O and As–O bonds have been estimated using the fraction of each species and the total number of Ge, Ga, As atoms in the glasses, as calculated from the density and molar weight of glasses. The results are summarized in Table 4 and show that the oxysulfide glass network consists of a larger number of Ge–O bonds as expected. It is interesting to point out that most of the As–S bonds persist upon increasing the oxygen content. This finding is consistent with the fact that arsenic has a stronger affinity for sulfur and a weaker affinity for oxygen when compared to germanium and gallium. Thus, in agreement with infrared spectroscopy, XPS shows the presence of oxygen atoms in the first coordination shell of all three glass-forming cations leading to a decrease in the number of pure cation-sulfide polyhedra in the oxysulfide network. Such a trend is consistent with the increase of the glass transition temperature in Table 1.

4. Conclusions

New oxysulfide glasses in the Ge–Ga–As system have been obtained by a two-step melting process. Gallium, introduced as Ga_2S_3, was found to improve the incorporation of oxygen in the glass network due to its relatively larger affinity for bonding with oxygen. We have shown that an increase of oxygen content decreases the cut-off wavelength and increases the glass transition temperature, T_g. Infrared and Raman spectroscopies were useful tools in the study of structural change induced by the progressive incorporation of GeO_2. The compositional dependence of the Raman, IR and XPS spectra suggests the presence of Ge–O, Ga–O and As–O bonds and the formation of mixed Ge-oxysulfide tetrahedral units such as GeO_3S, GeO_2S_2 or $GeOS_3$.

Table 3
Relative fraction of Ge, Ga and As atoms bonded to O and S as a function of z in the glass system $Ge_{18}Ga_5As_7S_{70-z}O_z$

Z	Relative fraction of various species					
	Ge-3d		As^{3+}(S)	As^{3+}(O)	Ga^{4+}(S)	Ga^{4+}(O)
	Ge^{4+}(S)	Ge^{4+}(O)				
5	88	12	77	23	71	29
12.5	73	27	75	25	49	51

Table 4
Number of X–S and X–O bonds/cm^3 (X = Ge, Ga and As) as a function z in the glass system $Ge_{18}Ga_5As_7S_{70-z}O_z$

z	Number of bonds/cm^3					
	Ge–S	Ge–O	As–S	As–O	Ga–S	Ga–O
5	6.43E+19	8.77E+18	2.19E+19	6.54E+18	1.44E+19	5.89E+18
12.5	5.62E+19	2.08E+19	2.25E+19	7.48E+18	1.05E+19	1.09E+19

Acknowledgments

This work has been supported by the National Science Foundation international grants EEC-0244109 and DMR-031208. Support was also provided by educational US and French grants, including the Agence Nationale de la Recherche (Grant ANR-05-BLAN-0212-01), the CNRS (PICS Grant 3179) and a FACE Grant from the French Embassy in the US. Partial support from the EC through the Marie Curie Actions—NANONLO project (MTKD-CT-2006-042301) is also acknowledged.

References

[1] L. Zan, L. Huang, C. Zhang, J. Non-Cryst. Solids 184 (1995) 1–4.
[2] H. Nasu, Y. Ibara, K. Kubodera, J. Non-Cryst. Solids 110 (1989) 229–234.
[3] P.M. Kumta, S.H. Risbud, Ceram. Bull. 69 (1990) 1977–1984.
[4] K. Nassau, D.L. Chadwick, J. Am. Ceram. Soc. 65 (1982) 197–202.
[5] E.F. Riebling, J. Mater. Sci. 9 (1974) 753–760.
[6] Y. Kim, J. Saienga, S.W. Martin, J. Non-Cryst. Solids 351 (2005) 1973–1979.
[7] N. Terakado, K. Tanaka, J. Non-Cryst. Solids 354 (2008) 1992–1999.
[8] C. Maurel, T. Cardinal, P. Vinatier, L. Petit, K. Richardson, F. Guillen, M. Lahaye, M. Couzi, F. Adamietz, V. Rodriguez, M. Bellec, L. Canioni, Mater. Res. Bull. 43 (2008) 1179–1187.
[9] Z.G. Ivanova, V.S. Vassilev, E. Cernoskova, Z. Cernosek, J. Phys. Chem. Solids 64 (2003) 107–110.
[10] E.I. Kamitsos, Y.D. Yiannopoulos, C.P. Varsamis, H. Jain, J. Non-Cryst. Solids 222 (1997) 59–68;
E.I. Kamitsos, Phys. Rev. B 53 (1996) 14659–14662.
[11] G. Lucovsky, F.L. Galeener, R.C. Keezer, R.H. Geils, H.A. Six, Phys. Rev. B 10 (1974) 5134–5146.
[12] K. Murase, T. Fukunaga, Y. Tanaka, K. Yakushiji, I. Yunoki, Physica B 117–118 (1983) 962–964.
[13] P. Boolchand, J. Grothaus, M. Tenhover, M.A. Hazle, R.K. Grasselli, Phys. Rev. B 33 (1986) 5421–5434.
[14] E.I. Kamitsos, J.A. Kapoutsis, G.D. Chryssikos, G. Taillades, A. Pradel, M. Ribes, J. Solid State Chem. 112 (1994) 255–261.

[15] L. Petit, N. Carlie, T. Anderson, M. Couzi, J. Choi, M. Richardson, K. Richardson, Opt. Mater. 29 (2007) 1075–1083.
[16] G. Lucovsky, Phys. Rev. B 6 (1972) 1480–1489.
[17] G. Lucovsky, R.M. Martin, J. Non-Cryst. Solids 8–10 (1972) 185–190.
[18] R.J. Kobliska, S.A. Solin, Phys. Rev. B 8 (1973) 756–768.
[19] E.I. Kamitsos, J.A. Kapoutsis, I.P. Cuelac, M.S. Iovu, J. Phys. Chem. B 101 (1997) 11061–11067.
[20] E.I. Kamitsos, Y.D. Yiannopoulos, M.A. Karakassides, G.D. Chryssikos, H. Jain, J. Phys. Chem. 100 (1996) 11755–11765.
[21] G.D. Papatheodrou, S.A. Solin, Solid State Comm. 16 (1975) 5–8.
[22] G. Srinivasarao, N. Veeraiah, J. Solid State Chem. 166 (2002) 104–117.
[23] L. Koudelka, M. Pisarcik, O.L. Baidakova, J. Mater. Sci. Lett. 8 (1989) 1161–1162.
[24] J. Heo, J.M. Yoon, S.Y. Ryou, J. Non-Cryst. Solids 238 (1998) 115–123.
[25] C. Julien, S. Barnier, M. Massot, N. Chbani, X. Cai, A.M. Loireau-Lozac'h, M. Guittard, Mater. Sci. Eng. B 22 (1994) 191–200.
[26] S. Barnier, M. Palazzi, M. Massot, C. Julien, Solid State Ionics 44 (1990) 81–86.
[27] A.M. Loireau-Lozac'h, F. Keller-Besrest, S. Benazeth, J. Solid State Chem. 123 (1996) 60–67.
[28] D. Ilieva, B. Jivov, G. Bogachev, C. Petkov, I. Penkov, Y. Dimitriev, J. Non-Cryst. Solids 283 (2001) 195–202.
[29] S.V.G.V.A. Prasad, G. Sahaya Baskaran, N. Veeraiah, Phys. Status Solidi (a) 202 (2005) 2812–2828.
[30] L. Petit, K. Richardson, B. Campbell, G. Orveillon, T. Cardinal, F. Guillen, C. Labrugere, P. Vinatier, M. Couzi, W. Li, S. Seal, Phys. Chem. Glasses 45 (2004) 315–321.
[31] R.M. Lazelle, P. O'Brien, D.J. Otway, J.H. Park, Chem. Mater. 11 (1999) 3430–3432.